

# Mode-selective coupler for wavelength multiplexing using $\text{LiNbO}_3$ :Ti optical waveguides\*

Research Article

Daniel Runde, Stefan Breuer, Detlef Kip<sup>†</sup>

*Institute of Physics and Physical Technologies, Clausthal University of Technology, Leibnizstr. 4, 38678 Clausthal-Zellerfeld, Germany*

Received 13 November 2007; accepted 4 March 2008

**Abstract:** A mode-selective directional coupler based on titanium in-diffused channel waveguides in lithium niobate is investigated. This coupler may be utilized as a key part of an add-drop multiplexer for dense wavelength division multiplexing in optical network nodes. The proposed coupler is based on evanescent coupling of the fundamental mode of a single-mode channel to the first higher mode of a parallel bi-modal waveguide. Our experimental results show that a compact directional coupler with coupling efficiencies larger than 90%, large bandwidth around 1550 nm, and with negligible polarization dependence can be realized using electro-optic lithium niobate substrates.

**PACS (2008):** 42.79.Gn; 42.79.Sz; 42.82.Bq; 42.82.Et

**Keywords:** integrated optics devices; lithium niobate • dense-wavelength division multiplexing (DWDM) • add-drop multiplexer

© Versita Warsaw and Springer-Verlag Berlin Heidelberg.

## 1. Introduction

The possibility to transfer light power from one optical waveguide to another is a key functionality for numerous applications in integrated optics like switches, interferometers, and filters [1, 2]. For this purpose, directional couplers may be used, which rely on the extension of the evanescent electric field outside the guiding core region [1–8]. If the evanescent fields of two waveguides that are close enough to each other overlap, light power can be coupled between the two interacting modes. Experimen-

tally, directional couplers for light splitting purposes can be realized in a standard way using tapered optical fibers with a fixed interaction length before separation. However, the concept of directional couplers is also ideally suited to a planar geometry, which allows for the fabrication of couplers with tailored properties in various materials. Examples include broadband operation in a larger wavelength range for optical communications, fast electrical switching, polarization and mode-selective coupling, and intensity-dependent couplers that make use of nonlinear substrate material properties [5–8]. Besides semiconductors like silicon and III/V compounds, lithium niobate ( $\text{LiNbO}_3$ ) is considered one of the most promising materials for integrated optical devices. This is due to both, excellent linear and nonlinear optical material properties, and well-established techniques for waveguide formation.

\*Presented at 9-th International Workshop on Nonlinear Optics Applications, NOA 2007, May 17–20, 2007, Swinoujście, Poland

<sup>†</sup>E-mail: d.kip@pe.tu-clausthal.de

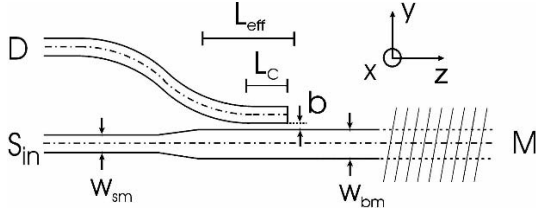


**Figure 1.** Scheme of the mode-selective coupler.  $S_{in}$ : single-mode waveguide input;  $D$ : drop port;  $M$ : output port;  $w_{sm}$  and  $w_{bm}$ : width of single- and bi-mode channels;  $b$ : inter-waveguide separation;  $L_C$ : coupler length;  $L_{eff}$ : effective coupler length. The tilted Bragg grating on the right hand side is for illustrative purposes only.

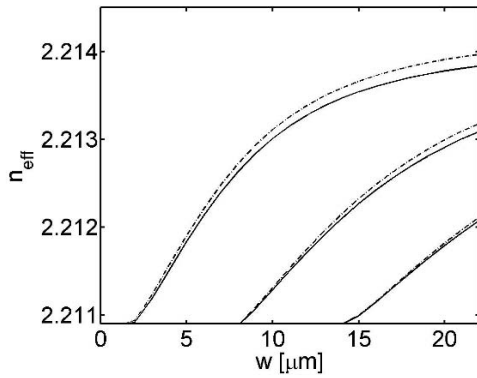


**Figure 2.** Mode dispersion of the first three modes (TE [---] and TM [—]) as a function of the width of titanium stripes (before in-diffusion). The ordinary substrate index is  $n_{sub} = 2.2109$ .

In this contribution, we present a mode-selective coupler in LiNbO<sub>3</sub> for application in an add/drop multiplexer for DWDM (dense wavelength division multiplexing) [9, 10]. In such a device, either a tilted or an asymmetric Bragg grating reflects a certain wavelength channel out of an input multi-channel data stream to a drop channel [11]. Spatial separation of the reflected signal from the input is realized by a mode-selective directional coupler, which is schematically depicted in Fig. 1. The multi-wavelength input signal is in-coupled at port  $S_{in}$  into a single-mode waveguide channel. The propagating light then adiabatically transforms in a tapered region into the fundamental mode of a wider, bi-modal waveguide section. Here, a tilted or asymmetric Bragg grating couples the input mode to the next higher reflected mode. The directional coupler is resonant for this higher mode and extracts the reflected signal of wavelength  $\lambda_i$  to the drop port  $D$ . Since the coupling efficiency in a real device will be lower than that of the asymmetric coupler considered here, the taper is also used to get rid of back reflected light in the unwanted

mode.

Bragg gratings in LiNbO<sub>3</sub> with sub-micron periods can be formed by lithographic patterning and etching of surface layers on top of the bi-modal waveguide section [13]. Alternatively, we have shown that holographic recording of elementary gratings using two-beam interference is an appropriate and efficient technique to record narrow-band reflection gratings using the photorefractive effect in LiNbO<sub>3</sub> [14, 15]. Compared to other optical materials like glasses or polymers, a multiplexer of the described scheme in LiNbO<sub>3</sub> allows for additional fast electrical switching of the Bragg grating in the GHz regime due to the superior electro-optic properties of this substrate material. In these systems, switching time constants are usually limited to the order of milliseconds [16, 17].

## 2. Modeling of the directional coupler

We modeled coupler properties with respect to low optical loss of tapered and bended waveguide sections, adequate (short) coupling length, high and asymmetric coupling efficiency, low polarization dependence, and wavelength independent operation in a large wavelength region. For this purpose, experimental parameters of the waveguide fabrication process are thickness  $d$  of the evaporated titanium film, width  $w$  of the lithographically patterned titanium stripes, and in-diffusion conditions (diffusion temperature  $T$  and time  $t$ ). With these values the two-dimensional diffusion profiles  $c_{Ti}(x, y)$  of titanium are calculated using literature data for the diffusion constant and index change  $\Delta n(c_{Ti})$  [15]. Then the wave equation is solved numerically for the resulting index profile  $\Delta n(x, y)$  by utilizing a finite difference method, resulting in the mode dispersion and the field distributions  $E(x, y)$  of the guided modes propagating in the  $z$ -direction. In Fig. 2 the mode dispersion of the first three modes of a channel waveguide versus the width of titanium stripes is plotted for  $\lambda = 1550$  nm,  $d = 100$  nm,  $T = 1273$  K, and  $t = 20$  h. The fundamental mode is guided for  $w > 2$   $\mu\text{m}$ , whereas the mode cut-offs of higher modes are at 8  $\mu\text{m}$  and 14  $\mu\text{m}$  for the second and third mode, respectively. For all following simulations a width of the titanium stripe of  $w_{sm} = 6$   $\mu\text{m}$  for single-mode waveguides and  $w_{bm} = 12$   $\mu\text{m}$  for the bi-modal waveguide sections are chosen.

The characteristics of the complete directional coupler are investigated using a three-dimensional beam propagation method (BPM) [18]. For the s-bend that is used to get a standard spatial separation of 127  $\mu\text{m}$  of the drop port from the input we chose an optimal length of 10 mm. The linear taper that connects the single mode section of width 6  $\mu\text{m}$

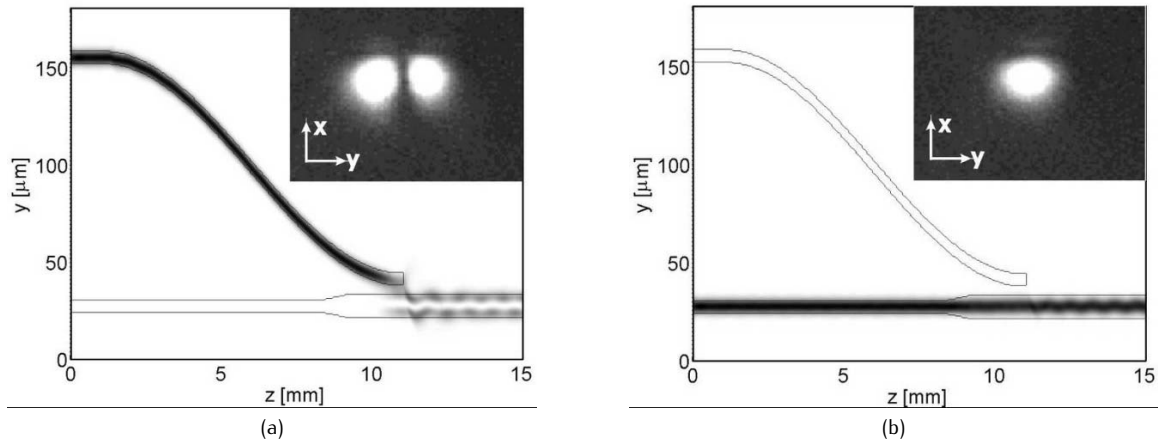


**Figure 3.** Simulated light propagation for light insertion into (a) drop port  $D$  and (b) input port  $S_{in}$ . The insets show the corresponding experimentally measured intensity distributions at the output port  $M$ .

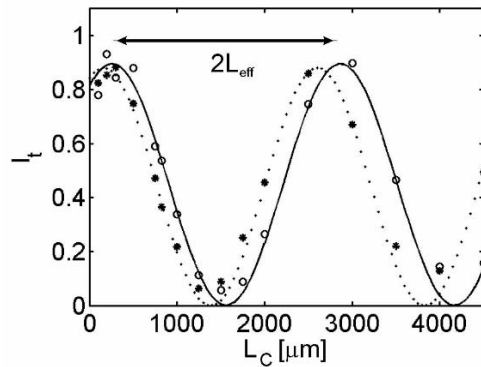


**Figure 4.** Measured characteristics of light transmission  $I_t$  from  $D$  to  $M$  versus interaction length  $L_C$  of the coupling area for TE (\*) and TM (O) polarization. The effective coupling length  $L_{eff}$  and maximum coupling efficiency  $\kappa$  are evaluated by fitting a  $\sin^2$  function to the measured data.

with the bi-modal  $12 \mu\text{m}$  wide channel is optimized to be  $1.5 \text{ mm}$  long. These parameters are fixed during the calculation of the coupler characteristics. As an example, in Fig. 3 the calculated light propagation for insertion into the drop port  $D$  [Fig. 3(a)] or into input  $S_{in}$  [Fig. 3(b)] is shown for an inter-waveguide separation of  $b = 5 \mu\text{m}$  and a coupler length  $L_C = 100 \mu\text{m}$  of the two parallel waveguides. In the overlap region of the two waveguides, light couples from the fundamental mode of the single-mode waveguide into the higher mode of the bi-modal waveguide. If light is inserted at  $S_{in}$  the mode transforms into the fundamental mode of the bi-modal channel. Because of the additional coupling among the bended drop channel waveguide and the straight bi-modal waveguide section

the effective coupling length  $L_{eff}$  for maximal power transfer can be significantly larger than  $L_C$ . From the ratio of out-coupled power at the output port  $M$  versus in-coupled power at ports  $S_{in}$  and  $D$ , respectively, the corresponding coupling efficiencies  $\kappa$  can be obtained. Maximal coupling efficiencies of  $\kappa \approx 0.65$  for the coupling efficiency from  $D$  to  $M$ , corresponding to coupler losses of about  $0.5 \text{ dB}$ , are found theoretically for inter-waveguide distances  $b$  around  $4 \mu\text{m}$ .

### 3. Experimental methods

From the simulation results different pre-optimized coupler structures are transferred onto a glass/chromium amplitude mask for lithography. For sample fabrication, pieces of  $(1 \times 7.8 \times 20) \text{ mm}^3$  are cut from  $x$ -cut wafers of optical-grade  $\text{LiNbO}_3$ . The  $c$ -axis is oriented parallel to the main waveguide direction along the  $20 \text{ mm}$  edge. In this geometry an effective holographic recording of Bragg gratings may be performed later for the development of an add/drop multiplexer [14]. Several coupler structures which differ in waveguide distance  $b$  and interaction length  $L_C$  are placed onto a single sample to reduce fabrication tolerances. In-diffusion of the patterned  $100 \text{ nm}$  thick Ti film takes place at  $1273 \text{ K}$  for  $20 \text{ hours}$  in a dry air atmosphere. After diffusion, facets of all samples are polished for light insertion via direct fiber coupling. The determination of effective coupling lengths and efficiencies is performed with the light of a single-longitudinal mode ECL laser providing wavelengths in the range  $\lambda = (1525 \text{ to } 1625) \text{ nm}$ . The polarized light of the laser is coupled either into input port  $S_{in}$  or drop port  $D$ , respectively, using single-mode polarization maintaining

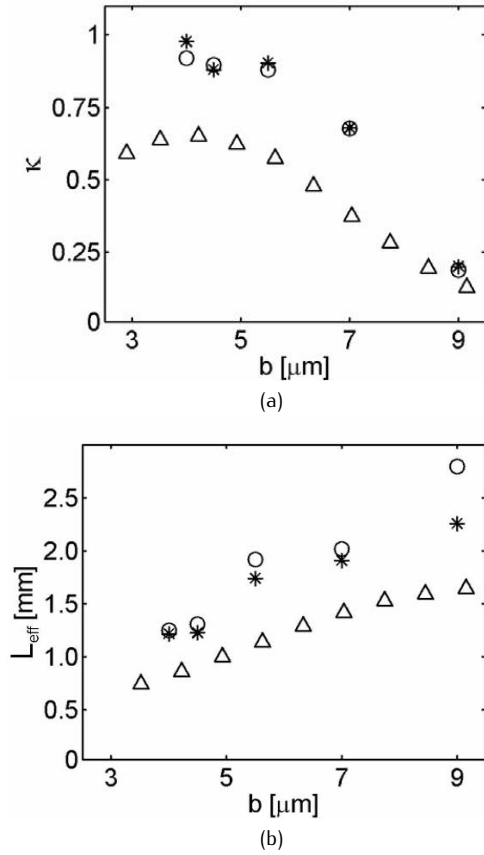


**Figure 5.** Comparison of simulated ( $\Delta$ ) and experimental [TE ( $*$ ), TM ( $\circ$ )] results for (a) coupling efficiency  $\kappa$  and (b) effective coupling length  $L_{\text{eff}}$  and as a function of inter-waveguide distance  $b$ .

fibers. An additional polarization controller allows for selective excitation of either TE or TM modes. The intensity distribution at the output  $M$  of the samples is monitored via a CCD camera. Input and output light powers are measured by fiber-coupled photo detectors.

## 4. Results and discussion

The principal operation of the coupler (with  $L_C = 100 \mu\text{m}$ ,  $b = 5 \mu\text{m}$ ,  $\lambda = 1550 \text{ nm}$ ) is shown in the insets of Fig. 3, where the intensity distribution on the output facet  $M$  has been measured. Light coupled to the input  $S_{in}$  remains in the pure fundamental mode also at the output  $M$ , whereas light inserted at the drop port  $D$  couples into the pure first higher mode of the bi-modal section. In both cases the second respective mode is completely suppressed below the sensitivity threshold of the used CCD camera. Estimated cross-coupling values are well below

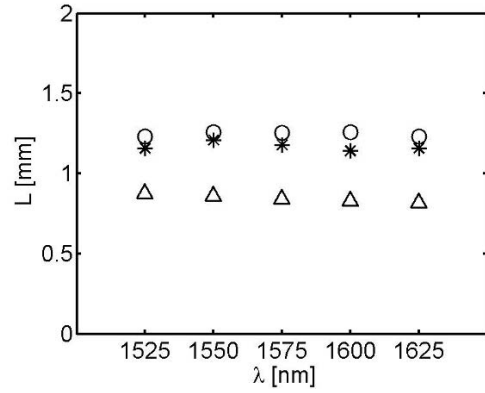


**Figure 6.** Wavelength dependence of a coupler with  $b = 4 \mu\text{m}$ . Experimentally-determined effective coupling lengths  $L_{\text{eff}}$  for maximum coupling of TE ( $*$ ) and TM ( $\circ$ ) modes are slightly higher than predicted by numerical results ( $\Delta$ ).

20 dB.

The effective coupling length  $L_{\text{eff}}$  can be determined by varying the interaction length  $L_C$  of the coupler design and measuring the coupling efficiency  $\kappa(L_C)$  for light propagating in the  $z$ -direction from  $D$  to  $M$ . The result for a coupler with  $b = 4.5 \mu\text{m}$  is shown in Fig. 4 for both TE and TM polarized input light. Effective coupling lengths and coupling efficiencies can be extracted from fitting a  $\sin^2$  function to the measured data. Obviously, light is already effectively coupled to the bi-modal waveguide section for a nominal coupler length  $L_C = 0$ . Experimentally, a maximum efficiency of about 90% is obtained for  $L_C = (0.25 \pm 0.02) \text{ mm}$ . This efficiency is significantly higher than values obtained by simulations, which may be attributed to the limited calculation window and necessary approximations used in BPM. An important result is the almost polarization-independent operation of the coupler for the shortest possible coupling length  $L_C$ . On the other hand, polarization sensitivity increases when using larger separations  $b$ : For larger values of  $b$  coupling lengths  $L_C$  have to be increased to obtain maximum coupling efficiencies, which implies larger total phase velocity differences of the two modes (see difference in transmitted  $I_t$  for  $L_C \approx 2.8 \text{ mm}$  of TE and TM modes in Fig. 4).

In Fig. 5 the measured coupling efficiency and effective coupler length are plotted as a function of inter-waveguide distance  $b$  for both TE and TM polarization. For comparison, the simulation results are also represented by triangles. Distances  $b < 3.5 \mu\text{m}$  are experimentally not suitable because titanium diffusion lateral to the surface will lead to partial fusion of the two channels. For such a situation our simulations show both, a decrease of coupling efficiency of the higher mode to the drop channel

[see values  $b \leq 4 \mu\text{m}$  in Fig. 5(a)] and also an increase of cross-talk resulting from coupling of the fundamental mode to the drop channel: cross-talk increases from  $-22$  dB ( $b = 4.5 \mu\text{m}$ ) to  $-13$  dB ( $b = 3 \mu\text{m}$ ) and  $-6$  dB. On the other hand, as expected, for increasing separations (and  $b \geq 4 \mu\text{m}$ ) the necessary coupling lengths  $L_{\text{eff}}$  increase from  $1.2$  mm ( $b = 4 \mu\text{m}$ ) to  $2.8$  mm ( $b = 9 \mu\text{m}$ ). At the same time the coupling efficiency  $\kappa$  is reduced from values close to one down to about 20% for the largest separation investigated here. To summarize, an inter-waveguide separation of  $b \approx 4.5 \mu\text{m}$  is a compromise yielding high coupling efficiency of the higher mode, while at the same time cross-talk from the fundamental mode and polarization dependence both remain moderately low.

For the application in DWDM networks, operation of the mode-selective coupler in a larger wavelength regime, for example in the full C-band, is required. Therefore, the coupler performance is measured as a function of input wavelength in the range of 1525 to 1625 nm. In Fig. 6 the obtained effective coupling length  $L_{\text{eff}}$  for maximum coupling efficiency  $\kappa$  shows only negligible wavelength dependence, in good qualitative agreement with simulation results.

## 5. Conclusions

An integrated-optical directional coupler as a key component of an add/drop multiplexer is demonstrated in lithium niobate. The coupler is based on selective evanescent coupling of the fundamental mode of a single-mode waveguide to the first higher mode of a bi-modal neighbored waveguide. High coupling efficiencies above 90% with high suppression of the undesired mode together with relatively short coupling lengths are obtained for small inter-waveguide separations. Our results show that the proposed coupler scheme in lithium niobate can be realized with low polarization and wavelength dependence. This opens the way for the development of integrated add/drop DWDM multiplexers that may use the superior electro-optic properties of this material suitable for fast electrical switching.

## Acknowledgement

Financial support from the Deutsche Forschungsgemeinschaft (KI 482/6-1/2) is gratefully acknowledged.

## References

- [1] R. Syms, J. Cozens, Coupled mode devices, In: Optical Guided Waves and Devices (McGraw-Hill Internat. Ltd., 1992) 1
- [2] R.V. Schmidt, R.C. Alferness, IEEE Trans. Circ. and Syst. 26, 1099 (1979)
- [3] W.P. Huang, J. Opt. Soc. Am. A 11, 963 (1994)
- [4] S. Lacroix, F. Gonthier, J. Bures, Appl. Opt. 33, 8361 (1994)
- [5] C.R. Doerr et al., IEEE Photonics Technol. Lett. 17, 1211 (2005)
- [6] K.Y. Song, I.K. Hwang, S.H. Yun, B.Y. Kim, IEEE Photonics Technol. Lett. 14, 501 (2002)
- [7] I. Kiyat, A. Aydinli, N. Dagli, IEEE Photonics Technol. Lett. 17, 100 (2005)
- [8] A. Villeneuve et al., Appl. Phys. Lett. 61, 147 (1992)
- [9] T. Erdogan, J.E. Sipe, J. Opt. Soc. Am. A 13, 296 (1996)
- [10] A. S. Kewitsch, G. A. Rakuljic, P. A. Wilems, A. Yariv, Opt. Lett. 23, 106 (1998)
- [11] H.S. Park, S.H. Yun, I.K. Hwang, S.B. Lee, B.Y. Kim, IEEE Photonics Technol. Lett. 13, 460 (2001)
- [12] J.M. Castro et al., Opt. Express 13, 4180 (2005)
- [13] J. Sochtig et al., Electronic Lett. 66, 333 (1998)
- [14] J. Hukriede, I. Nee, D. Kip, E. Krätzig, Opt. Lett. 23, 1405 (1998)
- [15] J. Hukriede, D. Runde, D. Kip, J. Phys. D: Appl. Phys. 72, R1 (2003)
- [16] Y.I. Zhu et al., Opt. Lett. 29, 682 (2004)
- [17] R. Asquini, J. D'Angelo, A. d'Alessandro, Mol. Cryst. Liq. Cryst. C 450, 403 (2006)
- [18] L. Thylen, E.M. Wright, G.I. Stegeman, C.T. Seaton, J.V. Moloney, Opt. Lett. 11, 739 (1986)